Heritage Science

RESEARCH

Open Access

Quantitative assessment of hardened leather artifact deterioration using infrared spectroscopy

Jingya Zhang[1], Lijuan Sun[1*] and Yuting Chen[1]

Abstract

This article describes a quantitative assessment method proposed to quickly identify the degree of deterioration of hardened leather artefacts. We used three techniques to artificially age samples, namely, dry-heat ageing (DH), UV-ageing (UV), and alkali-thermal ageing (AT). The deterioration mechanisms were studied via thermogravimetry/derivative thermogravimetry (TG/DTG) and attenuated total reflectance Fourier transform infrared spectroscopy (ATR-FTIR). Combined with amide III band deconvolution and second derivative fitting, we constructed a method for assessing the degree of deterioration by the relative content of random coils (referred to as R) in the secondary structure of the protein. The results show that with increasing ageing time, the macrostructures and microstructures of the leather changed to varying degrees. This study elucidates the differential behaviour of vegetable-tanned leather collagen under oxidative and hydrolytic mechanisms. Based on the deterioration characteristics and fitting results, we divided the hardened leather into the following three levels. Mild deterioration: $0 \le R \le 5\%$; leather with reduced pores and slight dryness and hardness but with a stable collagen structure; if the β-sheet content is ≥ 68% at this point, the leather may be recrosslinked by ultraviolet irradiation. Moderate deterioration: $6 \le R \le 25\%$; partial hydrogen bond breaking in leather, loosening of the collagen–tan matrix, dry and hard curling of the leather surface, and fibre cementation. Severe deterioration: $R \ge 40\%$, β-sheet ≤ 24%, and the α-helix is higher; surface reflection, severe macroscopic deformation and embrittlement, and the breakdown and gelatinization of the three-stranded helical structure of leather proteins. The quantitative analysis method was suitable for studying the deterioration mechanisms and assessing the degree of deterioration in Heishanling leather artefacts, which also provides a new practical scheme for assessing the degree of hardened leather.

Keywords Hardened leather, Deterioration, ATR-FTIR, Protein secondary structure, Ageing techniques

*Correspondence:
Lijuan Sun
slj329@163.com

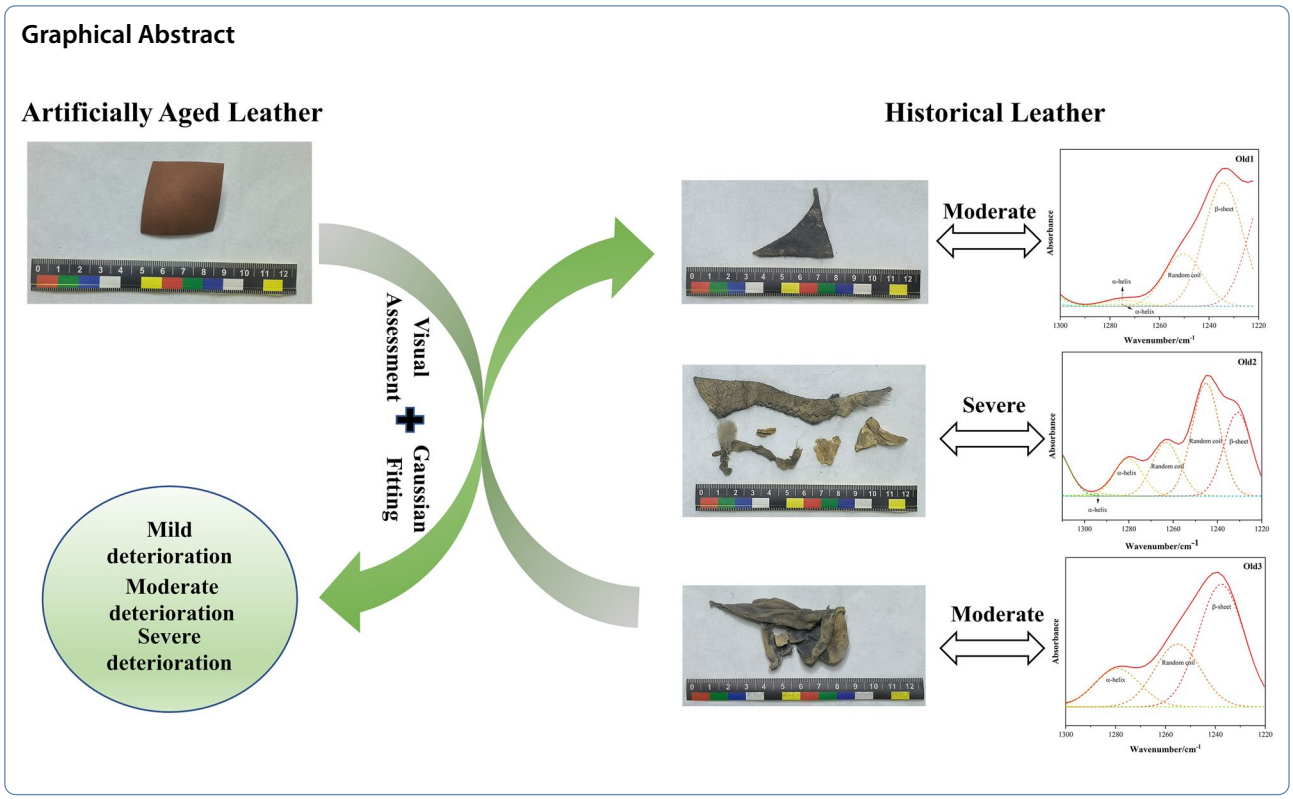

Introduction

Recently, interest in the use of scientific detection methods to study the mechanisms of leather deterioration and evaluate the degree of deterioration has increased. Leather is an organic substance that is made from animal hides through processes such as scraping, tanning, and finishing. Leather artefacts are a focus of worldwide research and have a rich and diverse history, encompassing items such as books, knives, and garments. As a natural polymer material, the internal complex components of leather are prone to different types of damage (deterioration, degradation and denaturation) due to factors such as temperature, humidity, light, pH, and microorganisms, causing irreversible changes from the macroscopic morphology to internal collagen structure. Numerous notable relics, including thirteenth century parchments [1] and ancient Egyptian leather objects and fragments from 2030 $_{BCE}$-364 $_{CE}$ [2], have deteriorated into dry, brittle and fragmented conditions. Incorrect extraction and preservation may lead to considerable losses. Therefore, timely and accurate diagnosis of leather artefact deterioration during excavations and the application of specific conservation techniques are crucial.

To date, few studies have evaluated the degree of leather deterioration. Most of these methods qualitatively evaluate leather objects by observing morphological and colour changes or quantitatively evaluate them by observing the percentage of fibre morphological damage or by using differential scanning calorimetry (DSC) deconvolution to study changes in the collagen structure [3]. The visual evaluation of qualitative damage involves subjective factors, and the results of quantitative analysis are more scientific and objective. For example, scanning electron microscopy (SEM) combined with morphological observations can be used to quantitatively evaluate the degree of deterioration of leather cultural relics, and K-means clustering analysis has been used to analyse the length and width of collagen fibres in parchments [4, 5]. Thermal analysis methods such as TG, DSC, microhot table (MHT), and dynamic mechanical analysis (DMA) have been used to analyse leather, which has attracted widespread attention [6–8]. Badea [6] used micro DSC to study the synergistic effect of temperature and relative humidity on parchment and divided four deterioration areas according to the deconvolution of the DSC denaturation peak. Carsote [7] further combined MHT to use the temperature range of the collagen structure distribution after DSC deconvolution to divide leather deterioration into leather-like (L) domains, parchment-like (P) domains, and gelatine-like (G) domains. Budrugeac [8] used TG/DTG, DSC, and MHT to analyse leather samples and a

large number of collagen-based materials in 16–17th century Romanian Brasov military coats and evaluated the qualitative damage to the leather samples. In addition, Zhang [9] used solid-state nuclear magnetic resonance (SSNMR) to quickly and quantitatively assess collagen degradation in archeological leather based on the relative amino acid content. Thermal analysis and solid-state NMR provide valuable insights into the structural changes in collagen, aiding in the understanding of leather deterioration and thermal degradation under various environmental conditions. However, these techniques are time-consuming and require combined analysis via MHT and DSC, limiting their practicality for excavated artifacts and samples needing immediate treatment. While amino acid content analysis can elucidate collagen degradation mechanisms, it involves costly and nonportable instrumentation.

Infrared spectroscopy, combined with chemometrics, hydrogen–deuterium exchange (HDX), and MHT, is widely used to analyse collagen microstructures in leather artefacts. These methods help determine deterioration mechanisms, assess deterioration levels, and evaluate preservation and restoration outcomes [10–15]. Vyskočilová 10 used FTIR-ATR spectroscopy and second-derivative analysis to observe the loosening of the collagen–tannin matrix, detanning processes, and the formation of gelatine. Gong [11] combined HDX with FTIR to study leather deterioration patterns, using deuterium exchange rates and characteristic peak shifts to characterize changes in collagen. Mehta [12] employed FTIR-ATR and Raman spectroscopy combined with chemometrics to analyse Gaussian fitting of the amide I band, enabling an assessment of changes in the secondary structure of collagen during leather processing. Ebersbach [13] employed infrared spectroscopy and MHT to study the deterioration of vegetable-tanned leather under different ageing conditions, identifying key deterioration types through amide band spacing and intensity ratios. Boyatzis [14] used infrared spectroscopy for peak fitting of the amide I and II bands, revealing collagen gelation phenomena in parchments treated with iron gall ink. Zhang [15] used FTIR to confirm that the deterioration of leather armour from the Yanghai cemetery resulted from damage to the triple helix structure. At the same time, the research on protein infrared spectroscopy in the field of biology mainly analyzes the behavior of amide I band and amide II band protein denaturation [16, 17]. FTIR has been widely confirmed as a reliable method for assessing the deterioration of leather artefacts through analysis of the amide I band. The amide III band is more suitable for quantitative analysis than the amide I band is because no interference from water or other overlapping peaks is detected [18]. The amide III band (1220–1330 cm^{-1}) has three collagen secondary structure types, including α-helices (1300–1270 cm^{-1}), random coils (1270–1240 cm^{-1}) and β-sheets (1240–1230 cm^{-1}) [15]. In contrast, few studies have used the amide III band to assess leather artefact deterioration. Zhang [15] investigated the differences in protein secondary structures of ancient leather compared with modern and artificially aged leather using the amide III band, characterizing the deterioration features of ancient leather. Lei [19] analysed the impact of photooxidation on the collagen structure via the amide III band. These studies validated the applicability of amide III band analysis for assessing leather deterioration.

Nearly all leather is "hardened", characterized by dryness and brittleness. Xinjiang has many kinds of leather cultural relics with a large age span, and the proportion of 'hardened' leather is very large. To facilitate rapid and accurate assessments at excavation sites, effective extraction and preservation strategies should be provided, and connections between the macro- and microscale phenomena of leather cultural relics should be established. We carried out the following experiments. We applied DH, UV, and AT ageing to modern vegetable-tanned sheepskin to simulate the impacts of arid and marshy environments on leather artefacts. A preliminary quantitative evaluation system for assessing the deterioration of leather artefacts was established, primarily based on the relative content of random coils in the secondary structure of the amide III band in the infrared spectra, and was applied to the study of Heishanling leather cultural relics. Compared with the amide I band method, the amide III band method can eliminate the influence of water and other overlapping peaks. It is a nondestructive or microdestructive method for quantitatively evaluating the degree of deterioration of hardened leather relics, which also aids in the assessment of other collagen-based materials.

Materials and methods

Materials

The studied samples were new leather, artificially aged leather, and historical leather. The chemicals used in the experiment were analytically pure. The artificial ageing samples were vegetable-tanned sheep leather tanned by researchers in 2016 at the Leather Base of Wenzhou University in Zhejiang Province, facilitating the control of experimental variables. Sheepskin is prevalent among historical leathers, and this study focused on collagen conformational changes during ageing, with findings applicable to other leather types. Thus, we selected sheepskin for its abundance, soft texture, fine-grained nature, and ease of processing. Vegetable tannage is the oldest and most representative tanning method, with

most leather produced from plant sources until the late nineteenth century [20]. According to Covington's tanning theory, collagen is initially linked to the surrounding aqueous matrix through multiple hydrogen bonds. Tannin molecules then crosslink with this structure, forming a macromolecular network around the triple helix, thereby increasing the stability of the leather [21, 22]. We selected raw hides from Xinji, Hebei (known as China's "Millennium Leather Capital"), and the commonly used natural tannin, Chinese bayberry tannin (condensed tannin), was used. Leather tanned with this agent has a lighter colour, closely resembling that of unprocessed leather artefacts. We also employed fish oil, Chinese bayberry tannin, and formic acid for retanning to achieve more uniform physical properties across the entire sheepskin. Since 2016, leather has been stored in a dry laboratory cabinet, where outdoor temperature and humidity fluctuations are relatively stable. The leather is free from damage and remains soft and fine, making it suitable for use as an unaged sample.

The Heishanling turquoise mining site in Lop Nor, Ruoqiang, Xinjiang (41°22′40"—41°1′55" N, 92°51′55"—93°4′11" E), is one of the largest and most significant turquoise deposits in China [23]. From 2016 to 2020, researchers conducted investigations and excavations that uncovered pottery, minerals, and organic materials. The site is located in an uninhabited area characterized by extreme aridity and high temperatures, with annual precipitation of 25 mm and evaporation exceeding 3000 mm [24]. The unique climatic conditions inhibit microbial growth and reduce decomposition rates, thereby effectively preserving easily degradable materials such as leather [25]. Excavated fur and leather products primarily include felt, leather mats, and fragments. By observing their morphology, they were identified and recorded as remnants of hats, insoles, and shoes [24]. The quantity of excavated leather has not been documented in detail. We selected three historical leather pieces, which were excavated and subsequently transferred to the laboratory for preservation in 2018 and 2019, designated old1, old2, and old3.

Methods

Leather ageing process

To ensure consistent performance, we cut 61 adjacent leather pieces (4 cm × 4 cm) along the dorsal spine of the same leather and divided them into 3 groups. Leather can be preserved in environments characterized by marshes, deserts, and dry-frozen environments [26]. During use and burial, leather artefacts may deteriorate due to light, temperature and humidity fluctuations, or pH. However, ageing experimental standards have yet to be established in leather artefact research. This study employed accelerated ageing methods to simulate leather artefacts from arid and marsh environments. Artificial samples subjected to DH and UV ageing were used to replicate the hardened leather artefacts found under dry conditions. First, the high temperatures associated with dry heat ageing accelerate the loss of moisture and oils within the leather while simultaneously disrupting the stable conformation of collagen. As a result, the leather becomes macroscopically dry, hard, and prone to brittleness [27]. Under controlled laboratory conditions, we used high temperatures to accelerate ageing, producing samples with significant visual differences for studying leather ageing patterns. Twenty samples were placed in a 120 °C electrothermal constant-temperature blast drying oven for 29, 55, 128, 201, and 274 h, respectively. Next, ultraviolet radiation can damage collagen structures, leading to peptide bond cleavage, compound degradation, and oxidative reactions, resulting in macroscopic hardening of the leather [28]. We treated 25 samples in a UV climate testing chamber (T = 50 °C, irradiance = 1–1.5 W/m^2, λUVA = 340 nm) for 48, 96, 144, 192, and 240 h, respectively [29]. Furthermore, a hydrolysis experiment was designed to verify the differences in collagen conformation changes between leather artefacts from marsh environments and those from arid environments. Marsh leather is particularly susceptible to pH fluctuations. Based on the alkaline immersion conditions observed in leather excavated from Valkenburg tombs in the Netherlands, we selected AT ageing [30]. This approach draws from commonly used alkaline treatment conditions in textiles, as leather shares a similar collagen-based material [31]. During this process, fibre swelling occurs from water absorption, leading to rapid protein deterioration due to reactions with alkaline substances. These results were compared with the results from the previous two experiments. Sixteen samples were immersed in 0.25 mol/L sodium hydroxide solution and placed in an electrothermal incubator at 60 °C for 1, 2, 3, and 4 h, respectively. The treated samples were dried in an incubator at 60 °C for 2 days. All the treated samples were kept in a glass desiccator for 48 h.

Ultra-depth 3D microscope

Visual assessment was performed via direct observation and an Ultra-Depth 3D Microscope KH-7700 (HORIX, Japan). After the white balance was adjusted, the surface morphology was recorded at magnifications of × 50 and × 100.

Thermal gravimetry/differential thermal gravimetry (TG/DTG)

TG/DTG curves were obtained via a TGA-DSC3 + instrument (Mettler Toledo, Switzerland) from 30 to 800℃, at a

20 ℃/min heating rate. Samples of approximately 5–7 mg were heated in alumina crucibles, with a volume of 70 µl, under high-purity nitrogen flow (50 ml/min). Origin 2017 software calculated the first derivative of the TG curve with respect to temperature/time (DTG curve).

Attenuated total reflectance fourier transform Infrared spectroscopy (ATR-FTIR)

ATR-FTIR measurements were performed with a TENSOR 27 instrument (Bruker, Germany). To preserve the leather samples, we used different measurement methods. Owing to the severe brittleness of the 4-h AT samples, a scissors and tweezers were used to collect fine fragments from the edges, which were then mixed with KBr at a 1:100 weight ratio. The mixture was pressed for 30 s under 15 MPa and placed in a window for determination, whereas the remaining samples were determined directly via ATR. The spectra were recorded via 16 scans in a range from 4000 to 600 cm^{-1} with a spectral resolution of 4 cm^{-1}. We measured six different points on both sides of each sample.

To obtain valid data, we adopted the following processing methods. OPUS software (Bruker, Germany) was used for preprocessing, such as smoothing, maximum and minimum normalization, water and carbon dioxide atmosphere compensation, and baseline correction. The smoothing parameter was set to 9, and the curves were saved. Origin 2017 software was used to convert the transmittance curve for analysis, with a parameter of 21. To obtain valuable data on the secondary structure of the collagen amide III band, the original absorbance spectra were saved in CSV format via OMNIC 8.2. Then, PeakFit v4 software was used for region selection, baseline correction, deconvolution, and second derivative fitting [32] to estimate the relative areas of the individual components in the amide III region. In the deconvolution period, Resp Fn Width was set to FWHM = 0.36024 to achieve stable, optimal Gaussian curves. The R^2 value was 0.97541651 or higher.

Results and discussion

Visual assessment

Figures 1, 2, 3 and 4 show representative macro images of the samples, highlighting significant differences among these groups. Compared with the new leather, all the artificially aged samples exhibited noticeable dryness and rigidity. During the ageing process, samples subjected to DH and UV irradiation presented a reduced pore size (Figs. 1, 2). Notably, in Fig. 1b–f, the fibre bundles of the grain surface in the DH samples were disordered, with irregular deformation observed at 201 h and 274 h (Fig. 1g, h). UV ageing was limited to irradiating the grains; thus, no changes were observed on the flesh side. The observed reduction in pore size may be attributed to the loss of internal components, leading to contraction of the leather. The AT samples were dry and brittle, with indistinguishable pore structures, a glossy surface, and significant curling and denaturation (Fig. 3). It is hypothesized that during the hydrolysis process, leather undergoes denaturation, resulting in rapid shrinkage and curling during drying. The increased gelatinization enhances surface glossiness [33]. Macro differences among the three sample groups may be related to varying deterioration mechanisms.

All three historical leather pieces were fragments (Fig. 4) that exhibit various types of deterioration in addition to hardening, making it impossible to distinguish the grain side. Old1 had a blue–black triangle

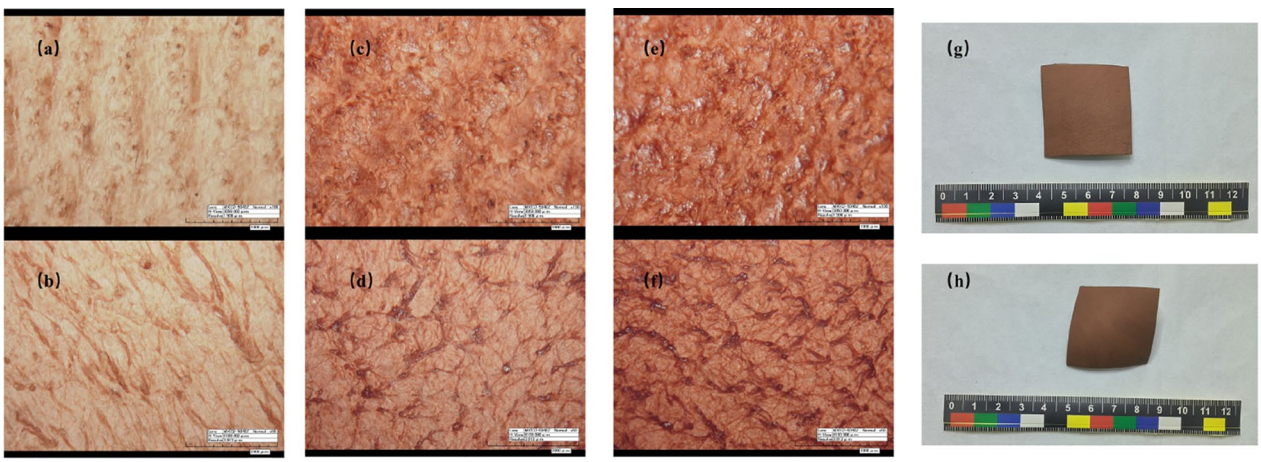

Fig. 1 Representative images from the visual assessment of DH samples. **a, c, e** 0 h, 29 h, and 274 h, respectively, grain growth control sides of leather × 100; **b, d, f** 0 h, 29 h, and 274 h, respectively, flesh sides × 50; and **g, h** deformed samples at 201 h and 274 h, respectively

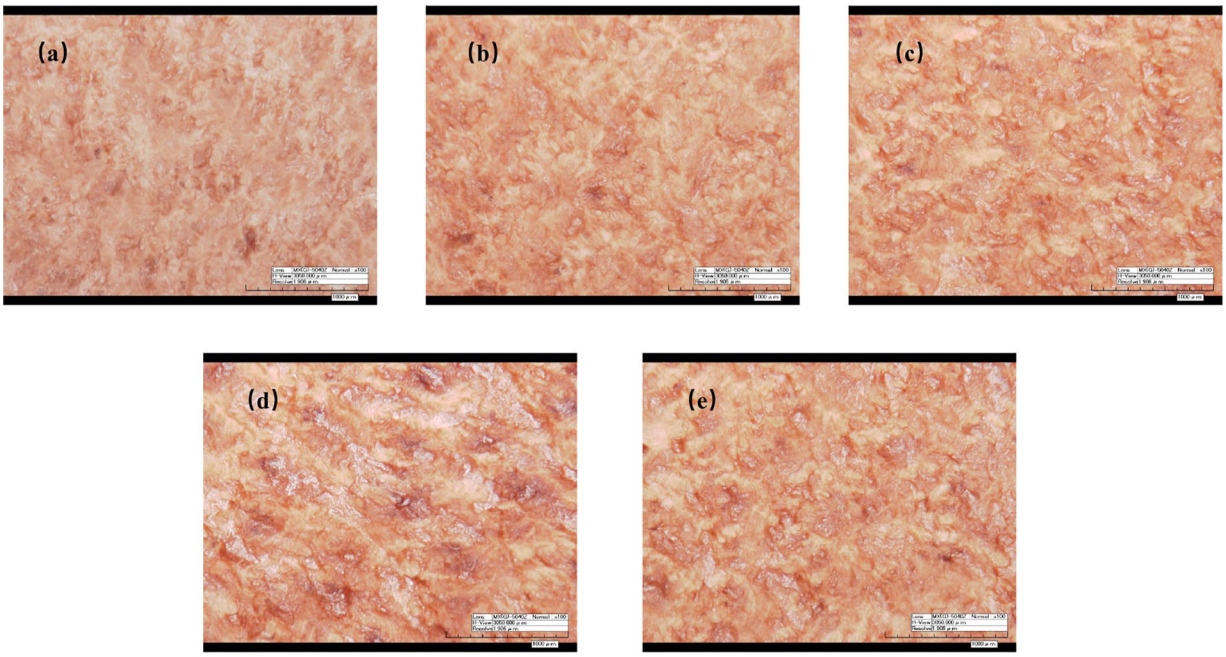

Fig. 2 Representative images from the visual assessment of UV samples. **a–e** Grain surfaces of leather at various stages × 100

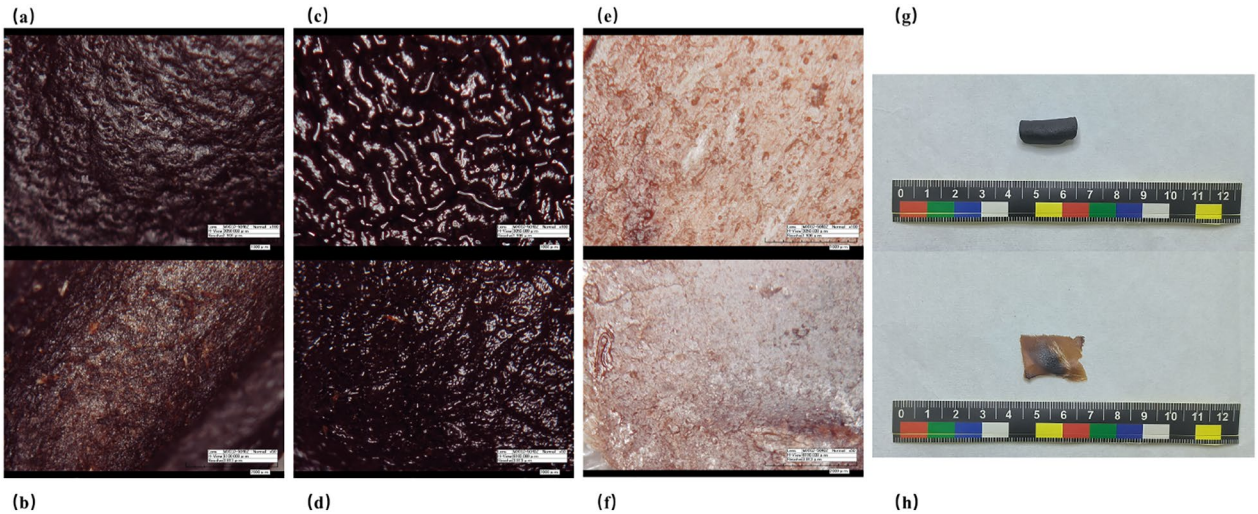

Fig. 3 Representative images from the visual assessment of AT samples. **a, c, e** 1 h, 2 h, and 4 h, respectively, grain growth control sides of leather × 100; **b, d, f** 1 h, 2 h, and 4 h, respectively, flesh sides × 50; and **g, h** crumpled and brittle samples at 1 h and 4 h, respectively

shape, the cross-section was neatly cut, and there was flaky white wear, fading, discolouration, and other imperfections. Old2 was broken into multiple pieces, with a blue–black slender shape, residual animal hair, mildew spots, decay, etc. Old3 was a yellow cyan–black soil flake, with an irregular gap in the middle, black soil particles, and obvious deformation and embrittlement.

Thermal stability analysis of artificially aged leather by TG/DTG

To further clarify the observed phenomena of dryness and curling in the visual assessment, we conducted TG/DTG analysis. We analysed the process of leather deterioration by comparing the changes in the maximum weight loss rate temperature and thermal degradation curve. The thermal degradation curve of leather can be divided into

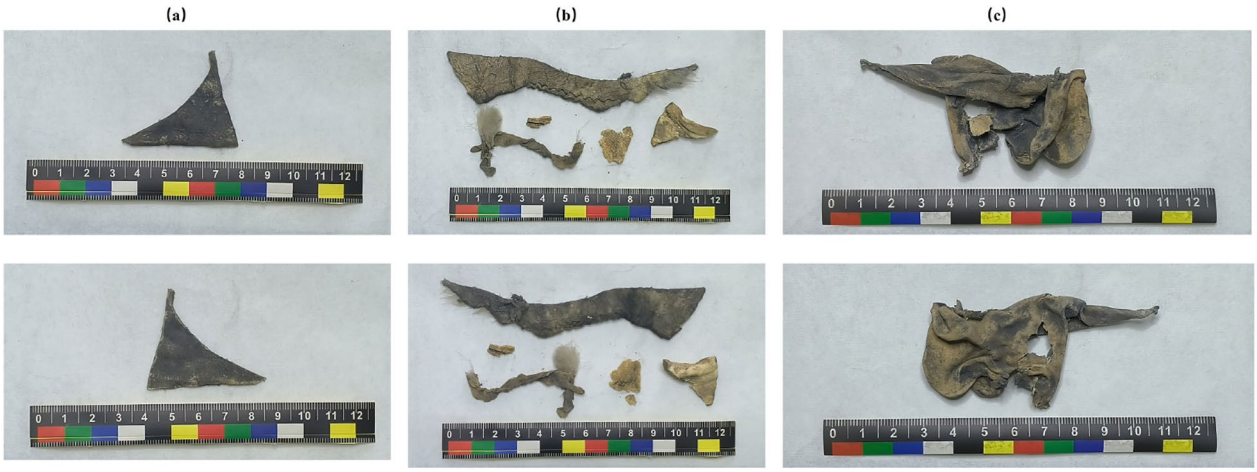

Fig. 4 Images from the visual assessment of historical leather. **a–c** Old1-Old3, respectively

three processes [10, 34]. The first process is dominated by the volatilization and loss of water and other small-molecule substances. The second stage is the main weight loss process, which includes the thermal degradation of protein components, lipids, etc. In this stage, the samples rapidly lose weight. Finally, the weight loss rate slows, which is a slow passive decomposition process of carbonaceous residue.

The TG/DTG curves in the first stage combined with the macroscopic phenomena indicate that the loss of water reduces the internal space of the samples, which leads to hardening. The thermal degradation curves of the DH and UV samples coincided with those of the new leather (Fig. 5a, e). The maximum weight loss rate temperature in the first process of DH was 69.21 °C (Table 1), and the DTG curve shifted upwards. The weight loss rate gradually decreased. The DTG curve of the UV samples also shifted to lower temperatures; this shows that the thermal stability of the leather and the water content were lower, which may be related to the destruction of the triple helix structure of the leather at high temperatures. The evaporation of bound water and free water accelerated the decomposition rate [34]. The temperature of the maximum weight loss rate was significantly prolonged in the first two AT processes, with the highest weight loss rate in each process (Fig. 5c, Table 1). There was more free water at first, indicating that the polypeptide chain was highly hydrolysed and that more hydrophilic groups were produced [35].

We can infer from the curve in the second stage that the formation and breaking of hydrogen bonds and changes in the helical structure of the collagen fibres led to an imbalance of stress in the samples, resulting in irregular deformation and curling. In the second process, the weight loss of the UV samples increased and then decreased, and the temperature of the maximum weight loss rate gradually increased. In addition, the temperature of the maximum weight loss rate of the DH samples was greater than that of the new leather; this may be due to the increased stability of collagen macromolecules remaining from the ageing process or associated with the denaturation of collagen [36]. In addition, Process 2 resulted in two distinct peaks in the AT samples, indicating the presence of two distinct protein conformations. Bozec [36] reported that the maximum weight loss rate temperature of collagen in Process 2 was 340 ± 10 °C, whereas the temperature of denatured collagen increased to 420 ± 10 °C. These findings indicate that collagen and gelatine coexist in the AT samples, which leads to an increase in the thermal degradation temperature and an increase in the weight loss rate. A substantial number of hydroxyl groups in the collagen and tanning agent molecules also release water molecules during the decomposition process, which increases the weight loss rate at the same time. In addition, the reduction in the amount of carbonaceous residue remaining at the end was also related to the presence of gelatine. Because gelatine does not contain tannins, the carbon residue produced during the thermal decomposition process is only the result of collagen decomposition [22]. This finding suggests that the reflective surface in the AT samples may result from severe collagen denaturation, with partial triple helix unravelling leading to gelatinization.

The temperature ranges corresponding to the three stages of new leather development were 30–164 °C, 164–516 °C, and temperatures above 516 °C, respectively. The weight loss rates were approximately 8.80%, 59.05%, and 15.31%, respectively (Table 1, Fig. 5). The weight loss rate of the artificially aged samples in the second process was greater than that of the new leather

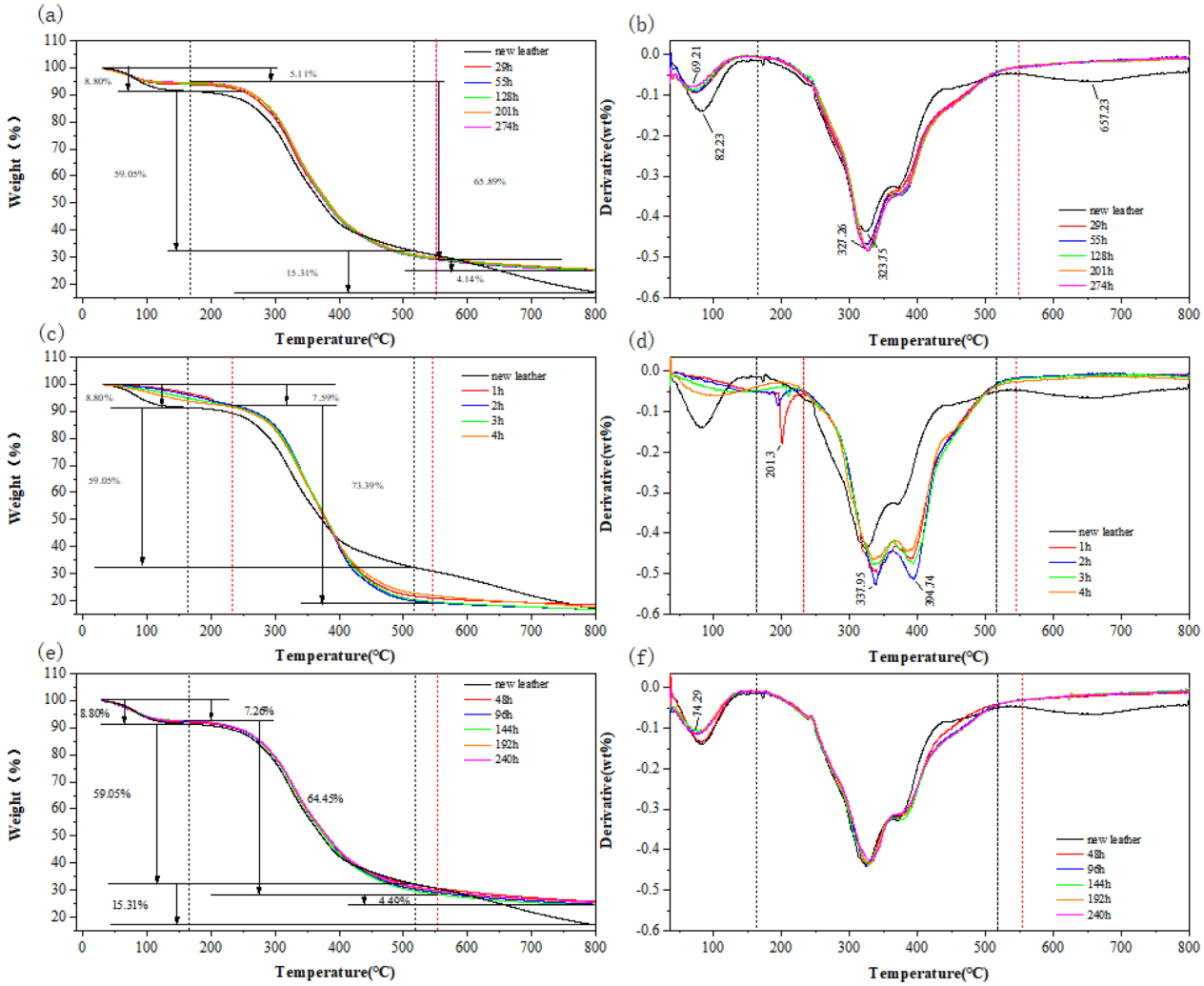

Fig. 5 TG/DTG curves obtained from artificially aged leather. **a, b** DH; **c, d** AT; and **e, f** UV

Table 1 TG/DTG parameters of leather samples before and after artificial ageing. Maximum weight loss rate with respect to temperature and weight loss rate in the three stages

Samples	I/°C	II/°C	III/°C	weight loss rate (I)/%	weight loss rate (II)/%	weight loss rate (III)/%	carbonaceous residue/%
New leather	82.23	323.75	657.23	8.80	59.05	15.31	16.98
DH	69.21	327.26	/	5.11	65.89	4.14	24.87
UV	74.29–82.23	323.75	/	7.26	64.45	4.49	24.40
AT	201.3	337.95–394.74	/	7.59	73.39	2.20	16.82

samples; this was possibly due to the reduced binding of collagen to tannins [29] or the loss of tannins accelerating the thermal decomposition process [37]. The samples retained consistent primary components across the ageing treatments, primarily reflecting the thermal degradation of collagen and the evaporation of volatile compounds. The similar pyrolysis and thermo-oxidation stages (the second process) in the TG curves align with the typical thermal behaviour [38] of collagen fibres; as polymers, they undergo depolymerization, random chain scission, and side group removal during thermal degradation. Moreover, visual assessment revealed that different conformational changes in collagen fibres, along with different

induction mechanisms, significantly affected the surface morphology.

Moreover, the DTG curves of the three artificially aged samples differ, which may be associated with oxidation and hydrolysis mechanisms. Research indicates that at a heating rate of 10 K/min, the rate of thermal degradation and oxidation ($d\%\Delta m/dt$) is closely related to the crosslinking of the collagen matrix. Moreover, lower rates correspond to greater degrees of deterioration [39]. In the oxidative mechanism, the continuously decreasing peak values of the DTG curves during AT suggest that prolonged ageing reduces crosslinking, indicating a loosening of the collagen–tannin matrix and a transformation of the collagen triple helix structure. The DTG curves for UV exhibit minimal differences, rendering this method unsuitable for comparison. However, AT samples subjected to hydrolytic conditions presented two distinct collagen states. Carşote [40] reported a similar occurrence of two collagen populations, indicating the coexistence of stable and unstable collagen. By comparing the thermal degradation behaviour of artificially tanned leather and parchment, they identified three processes in tanned leather: loosening of the collagen–tannin matrix, detanning, and collagen denaturation akin to parchment.

In summary, oxidation likely altered the collagen conformation without complete detanning, possibly due to the strong stability of condensed tannin–collagen [22]. However, alkaline hydrolysis accelerated detanning, leading to rapid collagen denaturation.

Analysis of molecular level changes in artificially aged leather by ATR-FTIR

We used ATR-FTIR to confirm the changes in the collagen structure at the molecular level. The main component of natural leather is protein, which contains more than 20 α-amino acids with the general formula R-CH(NH_2)-COOH and is connected by peptide bonds [41]. The main functional groups of α-amino acids include –CH_2-, –NH_2, and –COOH. N–H stretching vibration absorption occurs in the range of 3500–3300 cm^{-1}, and there is an absorption peak for amide A near 3424–3320 cm^{-1} [42]. The peaks at 2926 cm^{-1}, 2853 cm^{-1} and 1452 cm^{-1} correspond to the asymmetric stretching, symmetric stretching, and shear vibrations of CH_2-, respectively [41]. The amide I band is near 1644 cm^{-1}, which is the characteristic peak of the C=O stretching vibration and the strongest absorption band of proteins. The protein peptide is a sec-amide (R1-CONH-R2). The C=O stretching vibration frequency is located at approximately 1651 cm^{-1} when the protein secondary structure is dominated by α-helices and at approximately 1637 cm^{-1} when it is dominated by β-sheets. When the angular vibration of CNH in the secondary amide molecule is coupled with the C–N stretching vibration, it splits into two absorption peaks at 1560–1535 cm^{-1} and 1240 cm^{-1}. The former is mainly an NH in-plane variable angle vibration, known as the amide II band, which mainly appears at approximately 1550 cm^{-1}. The latter is mainly a C–N stretching vibration, known as the amide III band.

Figure 6a shows the infrared spectra of the new leather. The samples presented characteristic peaks near 3302 cm^{-1}, 1634 cm^{-1}, 1549 cm^{-1}, 1228 cm^{-1}, and 1030 cm^{-1}, corresponding to amide A, amide I, amide II, and amide III bands and C–O stretching vibrations, respectively. It is inferred that new leather might be dominated by β-sheets. All of the above peaks are consistent with the characteristic absorption peaks of new leather.

ATR-FTIR confirmed our hypothesis that oxidation leads to stable conformation disruption and loosening of the collagen–tannin matrix. Additionally, these findings suggest potential recrosslinking in the UV samples. Compared with those of the new leather samples, the amide A, amide I, amide II and amide III bands of the DH samples all shifted to lower wavenumbers (Fig. 6b). The amide A and amide II bands after UV irradiation for 48 and 240 h were the same as those described above (Fig. 6d). It has been reported that the peak shift of the amide band may be related to the stability of the hydrogen bond [43], indicating that the amide bond hydration is lower, the hydrogen bond is destroyed or there is a weak hydrogen bond, resulting in damage to the collagen triple helix structure. In addition, the loss of lipids and tannins in samples during DH, as well as the cleavage of hydrophobic bonds and hydrogen bonds between tannic acid and collagen, was observed. Tannins were oxidized and decomposed into small molecular compounds, such as the characteristic peak of lipid long-chain hydrocarbons near 2853 cm^{-1} and the peak of esters in tannins near 1030 cm^{-1} [44]. However, the amide I band of the UV samples and the amide II band at 144 h shifted to higher wavenumbers. It is inferred that the partially broken hydrogen bonds were regenerated, which maintained the pore size to a certain extent; this may be related to the destruction of the triple helix structure and the shrinkage of the leather, resulting in a decrease in the spacing of the molecular chains. More hydrogen bonds crosslinked to the body structure, supporting the mechanical stability of the leather.

ATR-FTIR confirmed the presence of multicomponent collagen in the AT samples, which was attributed to hydrogen bonding and peptide bond cleavage, along with conformational rearrangement. The structure of the collagen in the AT samples (Fig. 6c) changed most significantly after 2 h, and the amide A, amide I, and amide II bands all disappeared. After that, with increasing ageing time, the amide I and III bands shifted

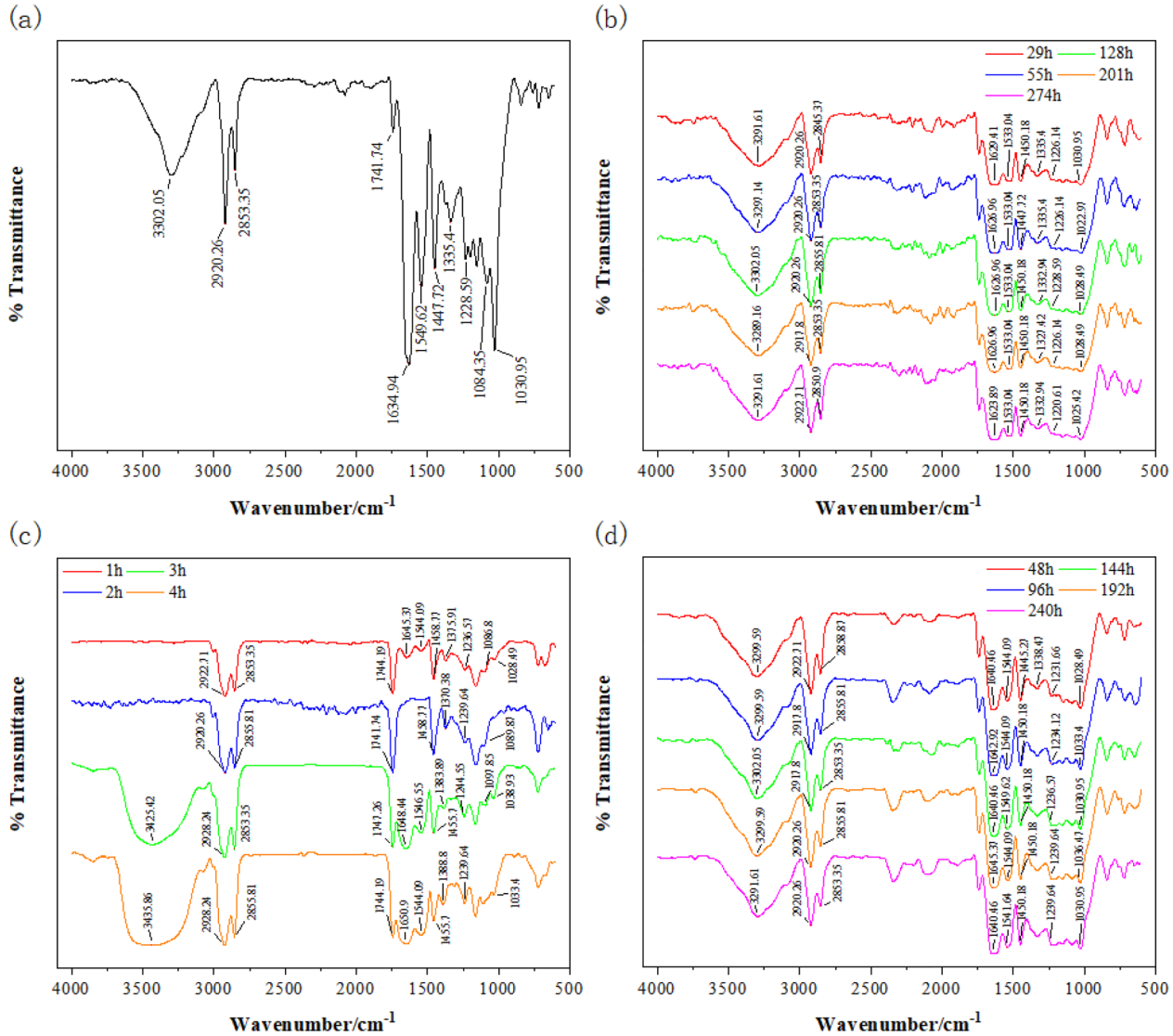

Fig. 6 ATR-FTIR spectra of new leather (**a**) and artificially aged leather. **b** DH; **c** AT; and **d** UV. The amide A, amide I, amide II, and amide III bands of collagen, as well as the fat liquoring oil bands, are in colour

to higher wavenumbers. This finding indicates that the hydrogen bond between N–H and C=O was first destroyed during the hydrolysis of collagen fibres [45] and that the protein was denatured. C = O was exposed to water, resulting in the fracture of collagen fibre peptide chains. The absorption peak at 1745 cm^{-1} might be the N-terminal and C-terminal residues formed by the free-peptide chains and might reduce the molecular weight of collagen [13], which affects the strength of the amide I and II bands. After the unwinding of collagen fibres, single-chain C=O groups are more likely to form hydrogen bonds than triple-helix structures [45], resulting in the reappearance of N–H stretching vibrational absorption peaks as well as the shift of amide I and III bands towards higher wavenumbers [46].

In summary, we found that macro- and microinteractions affect the deterioration process of hardened leather and that changes at the molecular level accelerate the development of macroscale phenomena. The breakage of hydrogen bonds and peptide bonds, as well as the destruction of the triple helix structure, led to denaturation of the protein and produced a gelatine-like structure. Therefore, the loss of leather components, dryness and hardness, deformation, curling, pore reduction, fibre cementation, and other phenomena continue to develop.

Quantification of deterioration

We analysed the changes in collagen according to the relative content of the secondary structure of the amide III band protein. This study further confirmed the presence of collagen denaturation, providing a reference for assessing the degree of leather deterioration. Table 2 lists the assignments and relative contents of different conformations in the amide III region of the artificially aged leather. The new leather was mainly composed of β-sheets, which is consistent with the previous analysis.

The relative content of random coils (R) in this study showed a consistent pattern, which can serve as a reference for assessing the degree of deterioration. An increase in this component indicates that the protein structure became more disordered, indicating denaturation. In the DH samples, the disordered components of collagen increased with ageing time, with the random coil content rising steadily, confirming earlier observations on the effects of DH. The deterioration of the UV samples may have occurred in the early stages of collagen deterioration, during which the triple helix structure transitioned to random coils, accompanied by moisture loss [47]. This process could have altered collagen–tannin binding and led to recrosslinking under prolonged irradiation. Notably, the random coil content in the UV samples at 48 h was significantly high, nearly reaching the levels observed in the late DH samples. The random coils subsequently disappeared, with only a slight presence at 192 h, corroborating earlier speculation regarding the reformation of hydrogen bonds. The collagen in the AT samples underwent significant denaturation, resulting in a markedly high content of random coils, confirming the earlier hypothesis.

Type I collagen is primarily composed of 33% glycine, 20–30% proline, and hydroxyproline, among others, according to species and tissue type [48]. The presence of consecutive amino acid residues with identical charges may generate electrostatic repulsion, leading to a low α-helix content (1%–3%), making detection challenging. However, the AT samples at 3 and 4 h presented a relatively high α-helix content, suggesting that protein denaturation induced conformational rearrangement, leading to the formation of stable ionic pairs of oppositely charged amino acid residues. The relative content of β-sheets had no distinct pattern, which was lower than that of unaged leather; this, in conjunction with the changes in α-helix content, suggests that some β-sheets disintegrated into random coils. Therefore, we used the relative content of the random coil (R) to determine the degree of deterioration.

In summary, based on these findings, we can construct a quantitative method to assess the degree of deterioration with the relative content of random coils (R) in conjunction with other components:

1) With mild deterioration ($0 \leq R \leq 5\%$), the pores of the leather shrunk, resulting in slight dryness, but the collagen structure remained stable. Additionally, the β-sheet content was $\geq 68\%$, which may be related to the recrosslinking of leather induced by ultraviolet exposure.

Table 2 ATR-FTIR spectral frequency and relative content of artificially aged leather in the amide III region

Samples	Ageing time/h	α-helix		Random coil		β-sheet	
		Frequency/cm^{-1}	Content/%	Frequency/cm^{-1}	Content/%	Frequency/cm^{-1}	Content/%
DH	0	1286	0.29	1247	3.46	1229	67.91
	29	/	/	/	/	1227	63.55
	55	1284	3.13	1242	15.80	1228	26.36
	128	1285	1.02	1245	13.15	1232	29.04
	201	1291	3.33	1243	21.08	1227	41.95
	274	1280, 1290	0.99	1258	24.90	1225	42.69
UV	48	1284	1.31	1244	17.24	1230	32.81
	96	1294	3.67	/	/	1228, 1232	70.14
	144	1286	1.55	/	/	1229	69.38
	192	1288	1.51	1242	4.48	1228	67.32
	240	/	/	/	/	1227, 1231	71.45
AT	1	/	/	1257,1267	10.80	1238	43.64
	2	/	/	1255, 1268, 1240	50.24	1227	3.82
	3	1276	9.19	1243,1258	44.34	1231	20.93
	4	1276	8.28	1242, 1250, 1258	53.45	1229	23.82

2) Moderate deterioration ($6 \leq R \leq 25\%$) and partial disruption of hydrogen bonds resulted in loosening of the collagen–tannin matrix and an increase in random structures, consequently causing the leather to become dry, deformed, and curled, along with fibre consolidation.
3) Severe deterioration (R and β-sheet $\leq 24\%$, high relative content of α-helix), disruption of hydrogen bonds and peptide linkages resulted in disintegration of the triple helical structure, contributing to the gelation of the leather. Macroscopically, leather had significant deformation and brittleness, accompanied by an increase in surface reflectivity.

Deterioration assessment of ancient leather

TG/DTG curves (Table 3, Fig. 7a, b) show that the thermal degradation processes of Old1 and Old3 were the same. The temperatures of the three processes were 30–200 °C, 200–574 °C, and above 574 °C, respectively, and the weight loss rates were approximately 12.66%, 56.27%, and 4–5%, respectively. However, the weight loss rates of the old2 samples were 10.62%, 41.82%, and 9.2%, respectively. The complete structure of the historical leather collagen was destroyed, and tannins and lipids were degraded.

In Fig. 7c, the amide A and amide II bands of Old1 moved to lower wavenumbers, and the peak area decreased significantly. The amide I and amide III bands shifted to higher wavenumbers. The characteristic peaks of tannins and lipids near 1741 cm^{-1}, 1084 cm^{-1} and 2853 cm^{-1} disappeared, whereas the characteristic peak of esters in tannins occurred near 1030 cm^{-1}; this means that the hydrogen bonds of the sample were broken, the lipids were lost, and the tannins decomposed into small molecules, but the single-chain C=O groups produced hydrogen bonds after the collagen fibres were unwound. The amide A, amide I, and amide II bands of Old2 all shifted to lower wavenumbers, but the amide III band shifted to a higher wavenumber; this might be related to the existence of weak hydrogen bonds after unwinding. Overall, the infrared spectrum of Old3 shifted to a higher wavenumber, the peak at 1741 cm^{-1} disappeared, and the peak at 1084 cm^{-1} decreased, indicating that the sample experienced less loss of lipids and tanning agents and that there were stronger hydrogen bonds.

The above methods cannot be used to determine the degree of deterioration of ancient samples; therefore, we used the methods established in this study to assess them (Fig. 8, Table 4):

(1) Old1 had moderate deterioration and was similar to the DH 55-h and 128-h samples. R = 8.69% and the β-sheet content was relatively low. These findings indicate that old1 exhibited partial hydrogen bond breakage, resulting in loosening of the collagen–tannin matrix and partial disintegration of the triple helix structure.
(2) Old2 had severe deterioration, which was similar to the AT samples. R = 26.81% and there was a high α-helix content and low β-sheet content, along with pronounced dryness and surface brittleness. This finding indicates that old2 may have experienced rearrangement and detanning following triple helix disintegration but has not yet transitioned to the dual-collagen component stage.
(3) Old3 had moderate deterioration, which was similar to that of the DH 201-h sample. R = 18.75%, β-sheet = 36.54%, and there was a high α-helix content. Old3 was dry and brittle, suggesting partial disintegration and rearrangement of the triple helix structure in the leather, resulting in the formation of stable ionic pairs among certain amino acid residues.

This study swiftly determined the degree of collagen deterioration in historical leather. Although there were minor discrepancies in numerical values compared with artificially aged leather, the findings align with the patterns of this research. These variations were likely due to the complex interplay of environmental factors that the historical leather had experienced, along with concurrent degradation, which merits further investigation. This study elucidates the distribution of

Table 3 TG/DTG parameters of ancient leather

Ancient samples	I/°C	II/°C	III/°C	weight loss rate (I)/%	weight loss rate (II)/%	weight loss rate (III)/%	carbonaceous residue/%
New leather	82.23	323.75	657.23	8.80	59.05	15.31	16.98
Old1	77.15	330.00	/	12.66	56.27	5.40	25.67
Old2	71.42	322.05	729.27	10.62	41.82	9.2	38.52
Old3	81.58	331.69	/	12.66	56.27	4.44	26.63

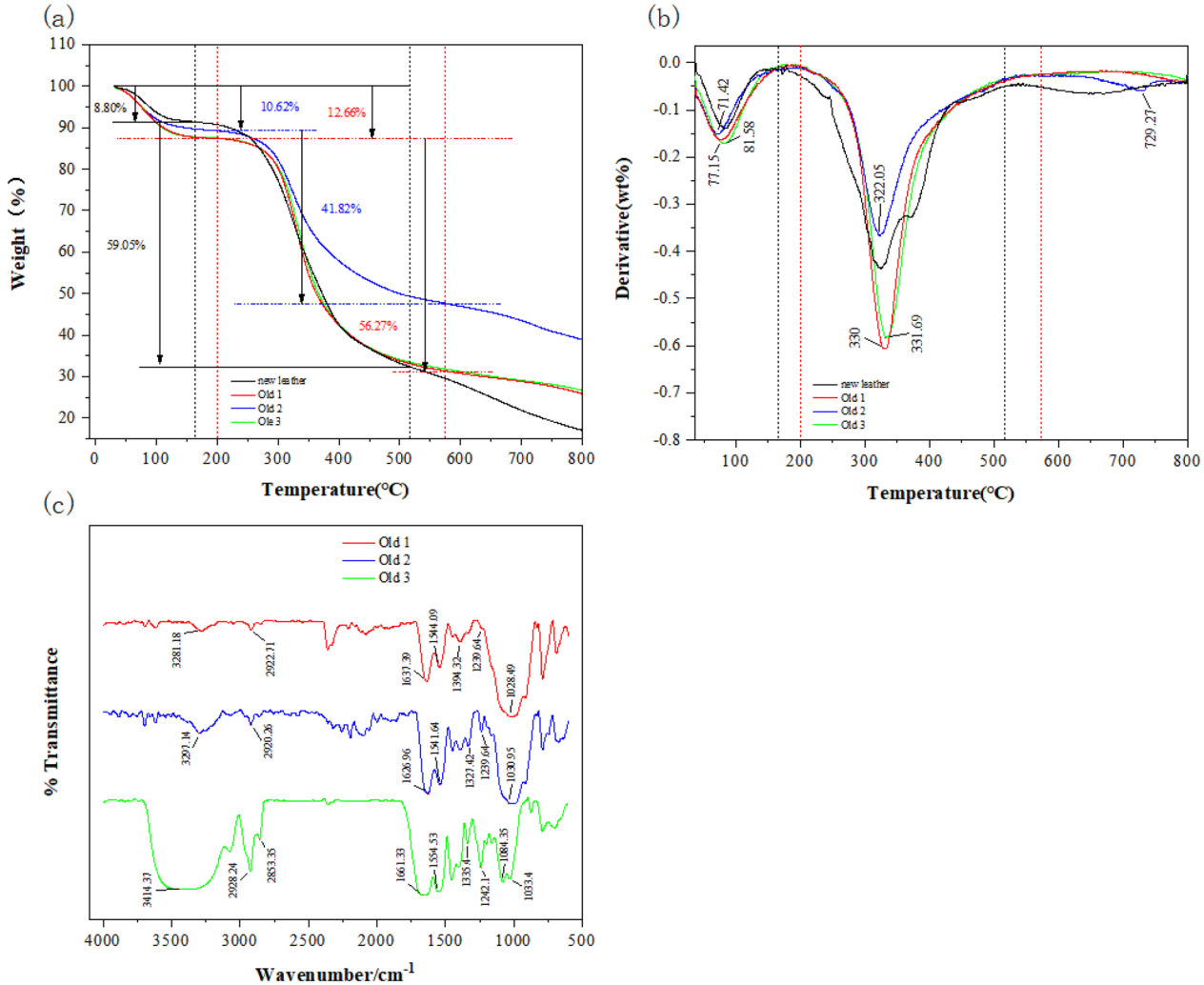

Fig. 7 TG/DTG curves and ATR-FTIR spectra of the ancient leather. **a** TG curves; **b** DTG curves; and **c** ATR-FTIR spectra

secondary structural components of vegetable-tanned leather but cannot confirm whether it has undergone degradation. In the future, it is still necessary to use high-performance liquid chromatography (HPLC) combined with this method for amino acid analysis to investigate the degradation of amino acids before complete disruption of the collagen conformation. Additionally, future studies should focus on the impact of tanning processes on crosslinking behaviour, analysing the developmental processes and underlying causes of repeated crosslinking.

Conclusions

The purpose of this study was to quantitatively evaluate the degree of deterioration of hardened leather via nondestructive or microdestructive analysis methods. A method for quantitative analysis of the relative content of random coils in the secondary structure of amide III band proteins based on infrared spectroscopy was initially utilized. The relationships between macro- and microdeterioration processes were determined, and the deterioration mechanisms of three ancient Heishanling samples were analysed to determine the degree of deterioration. The breakage of hydrogen bonds and peptide bonds in the hardened leather at the molecular level increased the disordered structure of the collagen fibres, resulting in protein gelation and denaturation, which aggravated the occurrence of a series of macroscopic deterioration events. Therefore, based on the relative content of R, hardening deterioration was divided into three grades: mild deterioration, moderate deterioration, and severe deterioration. The method was applied to artificially aged samples and ancient samples. This method can be applied to the analysis of fragile samples at archaeological sites. Researchers can obtain fitting data within minutes via portable infrared spectroscopy, allowing for

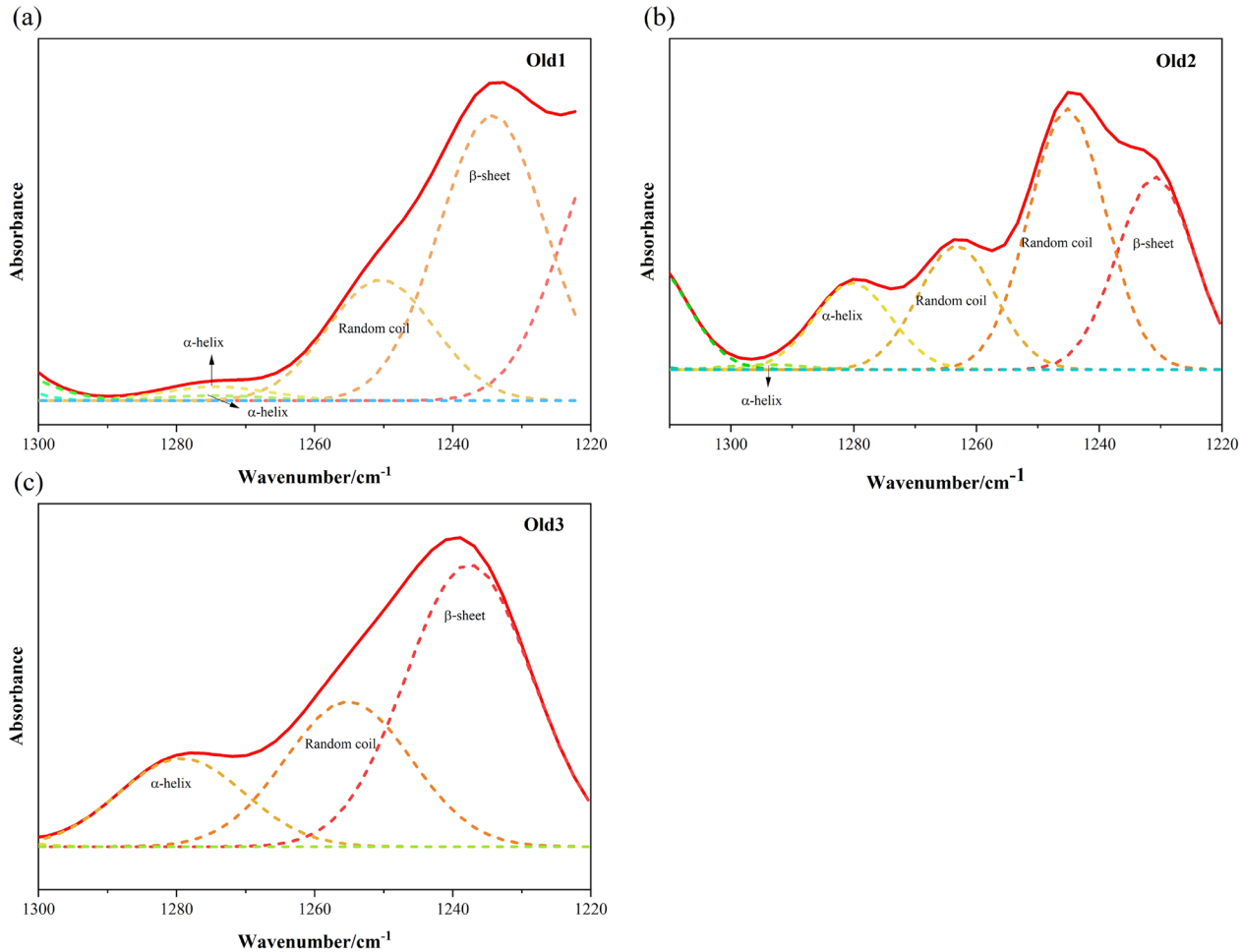

Fig. 8 Amide III curve-fitting spectra. **a** Old 1; **b** Old 2; and **c** Old 3

Table 4 FTIR spectral peak positions and relative contents of the ancient leather

Ancient samples	α-helix		Random coil		β-sheet	
	Frequency/cm^{-1}	Content/%	Frequency/cm^{-1}	Content/%	Frequency/cm^{-1}	Content/%
Old1	1274	1.36	1250	8.69	1234	20.56
Old2	1280,1294	6.39	1245, 1263	26.81	1230	13.41
Old3	1279	11.43	1255	18.75	1237	36.54

rapid assessment of collagen deterioration and enabling targeted temporary conservation measures. After further research and verification, it is believed that this quantitative method can be more widely used in the field of leather protection.

Abbreviations

ATR-FTIR	Attenuated total reflectance Fourier transform infrared spectroscopy
DH	Dry-heat
UV	Ultraviolet
AT	Alkali-thermal
TG	Thermogravimetry
DTG	Derivative thermogravimetry
and R	Random coil. DSC: differential scanning calorimetry
SEM	Scanning electron microscopy
MHT	Microhot table
DMA	Dynamic mechanical analysis
SSNMR	Solid-state nuclear magnetic resonance
HDX	Hydrogen–deuterium exchange
and HPLC	High-performance liquid chromatography

Acknowledgements

We thank Prof. Yiheng Xian for generously providing the ancient samples to verify the effectiveness of the method. The authors would also like to thank

Fellow Weiqiang Zhou for his support in providing us with the UV climate testing chamber and allowing us to obtain UV-ageing data in his laboratory.

Author contributions
JZ performed all the experimental work and wrote the manuscript. LS participated in the discussion of the experimental design and the process of manuscript revision. YC participated in the operating procedures for the ageing experiments and analytical tests. All the authors read and approved the final manuscript.

Funding
This research was provided by the project "Arrangement of archaeological data and research on the turquoise mining site of Heishanling, Ruoqiang, Xinjiang" supported by the National Office for Philosophy and Social Sciences in China.

Availability of data and materials
No datasets were generated or analysed during the current study.

Declaration

Competing interests
The authors declare no competing interests.

Author details
[1]School of Cultural Heritage, Northwest University, Xi'an 710127, P.R. China.

Received: 25 July 2024 Accepted: 13 November 2024
Published online: 12 December 2024

References

1. Lech T. Evaluation of a parchment document, the 13th century incorporation charter for the city of Krakow, Poland, for microbial hazards. Appl Environ Microbiol. 2016;82(9):2620–31.
2. Elnaggar A, Leona M, Nevin A, et al. The characterization of vegetable tannins and colouring agents in ancient Egyptian leather from the collection of the metropolitan museum of art. Archaeometry. 2017;59(1):133–47.
3. Badea E, Sommer DVP, Axelsson KM, et al. Damage ranking of historic parchment: from microscopic studies of fibre structure to collagen denaturation assessment by Micro DSC. Preserv Sci. 2012;9:97–109.
4. Vornicu N, Deselnicu V, Bibire C, et al. Analytical techniques used for the characterization and authentification of six ancient religious manuscripts (XVIII–XIX centuries). Microsc Res Tech. 2015;78(1):70–84.
5. Axelsson KM, Larsen R, Sommer DVP. Dimensional studies of specific microscopic fibre structures in deteriorated parchment before and during shrinkage. J Cult Heritage. 2012;13(2):128–36.
6. Badea E, Della Gatta G, Usacheva T. Effects of temperature and relative humidity on fibrillar collagen in parchment: a micro differential scanning calorimetry (micro DSC) study. Polym Degrad Stab. 2012;97(3):346–53.
7. Carsote C, Badea E. Micro differential scanning calorimetry and micro hot table method for quantifying deterioration of historical leather. Heritage Sci. 2019;7:1–13.
8. Budrugeac P, Carşote C, Miu L. Application of thermal analysis methods for damage assessment of leather in an old military coat belonging to the History Museum of Braşov—Romania. J Therm Anal Calorim. 2017;127:765–72.
9. Zhang Y, Li Y, Liu X, et al. Quantitative assessment of collagen degradation in archeological leather by solid-state NMR. J Cult Heritage. 2022;58:179–85.
10. Vyskočilová G, Carşote C, Ševčík R, et al. Burial-induced deterioration in leather: a FTIR-ATR, DSC, TG/DTG, MHT and SEM study. Heritage Sci. 2022;10(1):7.
11. Gong DC, Li Z, Wang ZX, Wei SN, Chen LX, Zhang Y. Research on the microstructure of collagen in ancient leather by hydrogen-deuterium exchange. Sci Conserv Archaeol. 2021;33(05):1–8. https://doi.org/10.16334/j.cnki.cn31-1652/k.20200501749(inChinese).
12. Mehta M, Liu Y, Naffa R, et al. Changes to the collagen structure using vibrational spectroscopy and chemometrics: a comparison between chemical and sulfide-free leather process. J Am Leather Chem Assoc. 2021;116(11):379–89.
13. Vyskočilová G, Ebersbach M, Kopecká R, et al. Model study of the leather degradation by oxidation and hydrolysis. Heritage Sci. 2019;7(1):1–13.
14. Boyatzis SC, Velivasaki G, Malea E. A study of the deterioration of aged parchment marked with laboratory iron gall inks using FTIR-ATR spectroscopy and micro hot table. Herit Sci. 2016;4:13.
15. Zhang Y, Chen Z, Wang C, et al. Studies of structure changes of archeological leather by FTIR spectroscopy. J Soc Leather Technol Chem. 2018;102(5):262–7.
16. Barth A. Infrared spectroscopy of proteins. Biochim Biophys Acta. 2007;1767(9):1073–101.
17. Doyle BB, Bendit EG, Blout ER. Infrared spectroscopy of collagen and collagen-like polypeptides. Biopolymers. 1975;14(5):937–57.
18. Fu FN, Deoliveira DB, Trumble WR, et al. Secondary structure estimation of proteins using the amide III region of Fourier transform infrared spectroscopy: application to analyze calcium-binding-induced structural changes in calsequestrin. Appl Spectrosc. 1994;48(11):1432–41.
19. Lei KX, Yang L. A study on the mechanism of photo-oxidation of leather relics. Sci Conserv Archaeol. 2024;36(04):40–9. https://doi.org/10.16334/j.cnki.cn31-1652/k.20221102761(inChinese).
20. An H, Ma YR, Xie SB. Studies on the Leather-tanning Technique of the Ancient Europe. Relics Museol. 2018;06:80–6.
21. Covington, T. Tanning chemistry: the science of leather. Royal Society of Chemistry; 2009.
22. Sebestyén Z, Jakab E, Badea E, et al. Thermal degradation study of vegetable tannins and vegetable tanned leathers. J Anal Appl Pyrolysis. 2019;138:178–87.
23. Xiaoli Q. Turquoise ornaments and inlay technology in ancient China. Asian Perspectives. 2016;208–239.
24. Li YX, Yu JJ, Xian YH. A Survey of the Ancient Turquoise Mining Site at Heishanling in Ruoqiang, Xinjiang. Cultural Relics. 2020;(08):4–13+1.https://doi.org/10.13619/j.cnki.cn11-1532/k.2020.08.001(in Chinese).
25. Zhang M, Fan J, Liu J, et al. A comprehensive evaluation of a historical leather armor from Yanghai Cemetery, Turpan. Herit Sci. 2024;12(1):162.
26. Groenman-van Waateringe W, Kilian M, Van Londen H. The curing of hides and skins in European prehistory. Antiq. 1999;73(282):884–90.
27. Zhang YJ, Xi L, Hu XJ, et al. Protection and restoration of leather cultural relics excavated from Wayan Reservoir in Qinghai Province. Steppe Cult Relics. 2019;01:103–14. https://doi.org/10.16327/j.cnki.cn15-1361/k.2019.01.017(inChinese).
28. Tyan YC, Liao JD, Klauser R, et al. Assessment and characterization of degradation effect for the varied degrees of ultra-violet radiation onto the collagen-bonded polypropylene non-woven fabric surfaces. Biomaterials. 2002;23(1):65–76.
29. Yanping GAO, Shuang Y, Xiaoyun J, et al. Effect of UV irradiation on vegetable tanned leather. Rev Pielarie Incaltaminte. 2015;15(4):219.
30. Sun X, Yang HL, Zhou Y. Research on the archaeological distribution and technique characteristics of foreign leather artifacts. J Silk. 2024;61(06):149–58 **(in Chinese)**.
31. Zhang XM, Yuan SX. Analytical research on aged silk by SEM. J Chin Electr Microsc Soc. 2003;05:443–8 **(in Chinese)**.
32. Liu K, He Y, Wang Z, Ma C, Yuan X, Yu X. Progress in determination of protein secondary structure by Fourier infrared spectroscopy and Raman spectroscopy. Food Ferment Ind. 2023;49(10):293–8. https://doi.org/10.13995/j.cnki.11-1802/ts.031883.
33. Acosta S, Jiménez A, Cháfer M, et al. Physical properties and stability of starch-gelatin based films as affected by the addition of esters of fatty acids. Food Hydrocoll. 2015;49:135–43.
34. Zhang Y, Liu XG, Yin H, Chen HJ, Yang NJ, Gong DC. Research on the degradation mechanism of archaeological leather using TG-FTIR and Py-GC/MS. Sci Conserv Archaeol. 2020;32(05):1–10. https://doi.org/10.16334/j.cnki.cn31-1652/k.2020.05.001(inChinese).
35. Sebestyén Z, Badea E, Carsote C, et al. Characterization of historical leather bookbindings by various thermal methods (TG/MS, Py-GC/MS, and micro-DSC) and FTIR-ATR spectroscopy. J Anal Appl Pyrolysis. 2022;162: 105428.

36. Bozec L, Odlyha M. Thermal denaturation studies of collagen by microthermal analysis and atomic force microscopy. Biophys J. 2011;101(1):228–36.
37. Liu D, Qiang XH, Li Y, Cui L. Effect of chrome/aluminum tanning agent retanning on the thermal Effect of chrome/aluminum tanning agent retanning on the thermal. J Shaanxi Univ Sci Technol. 2018;36(05):6–13. https://doi.org/10.19481/j.cnki.issn2096-398x.2018.05.002(inChinese).
38. Yang P, He X, Zhang W, et al. Study on thermal degradation of cattlehide collagen fibers by simultaneous TG–MS–FTIR. J Therm Anal Calorim. 2017;127:2005–12.
39. Budrugeac P, Cucos A, Miu L. The use of thermal analysis methods for authentication and conservation state determination of historical and/or cultural objects manufactured from leather. J Therm Anal Calorim. 2011;104(2):439–50.
40. Carşote C, Badea E, Miu L, et al. Study of the effect of tannins and animal species on the thermal stability of vegetable leather by differential scanning calorimetry. J Therm Anal Calorim. 2016;124:1255–66.
41. Zhang Y, Gong DC, Yang ZH, Huang WC. Identification of waterlogged leather unearthed from a Warring States Period tomb in Yiyuan, Shandong Province. Sci Conserv Archaeol. 2015;27(01):59–64. https://doi.org/10.16334/j.cnki.cn31-1652/k.2015.01.009(inChinese).
42. Doyle BB, Bendit EG, Blout ER. Infrared spectroscopy of collagen and collagen-like polypeptides. Biopolymers. 1975;14(5):937–57.
43. Sendrea C, Carsote C, Badea E, et al. Non-invasive characterisation of collagen-based materials by NMR-mouse and ATR-FTIR. Sci Bull B Chem Mater Sci UPB. 2016;78:27–38.
44. Dickinson E, High KE. The use of infrared spectroscopy and chemometrics to investigate deterioration in vegetable tanned leather: potential applications in heritage science. Heritage Sci. 2022;10(1):65.
45. Jiang Y, Wu P. Application of Near-Infrared Spectroscopy in the Study of Protein and Polymers with Amide Group. Prog Chem. 2008;20(12):2021–33.
46. Zhang C, Ren Z, Yin Z, et al. Amide II and amide III bands in polyurethane model soft and hard segments. Polym Bull. 2008;60:97–101.
47. Rabotyagova OS, Cebe P, Kaplan DL. Collagen structural hierarchy and susceptibility to degradation by ultraviolet radiation. Mater Sci Eng C. 2008;28(8):1420–9.
48. Bicchieri M, Monti M, Piantanida G, et al. Non-destructive spectroscopic characterization of parchment documents. Vib Spectrosc. 2011;55(2):267–72.

Publisher's Note